Available online at www.sciencedirect.com

ScienceDirect

Energy Procedia 126 (201709) 1011–1018

Energy Procedia

www.elsevier.com/locate/procedia

72nd Conference of the Italian Thermal Machines Engineering Association, ATI2017, 6–8 September 2017, Lecce, Italy

Numerical investigation of the performance of Contra-Rotating Propellers for a Remotely Piloted Aerial Vehicle

Maria Grazia De Giorgi[a,*], Teresa Donateo[a], Antonio Ficarella[a], Donato Fontanarosa[a], Anna Eva Morabito[a], Luca Scalinci[a]

[a] *University of Salento, Dep. of Engineering for Innovation, Via per Monteroni, 73100-Lecce, Italy*

Abstract

The present work aims at the numerical prediction of the performance of a Contra-Rotating Propellers (CRP) system for a Remotely Piloted Aerial Vehicles (RPAV). The CRP system was compared with an equivalent counter-rotating propellers configuration which was set by considering two eccentric propellers which were rotating at the same speed. Each contra-rotating test case was built by varying the pitch angle of blades of the rear propeller, while the front propeller preserved the original reconstructed geometry. Several pitch configurations and angular velocities of the rear propeller was simulated. Comparisons showed an improvement of the propulsive efficiency of the contra-rotating configuration in case of larger pitch angles combined with slower angular velocities of the rear propeller.

Peer-review under responsibility of the scientific committee of the 72nd Conference of the Italian Thermal Machines Engineering Association

Keywords: RPAV, aeronautic propulsion, performance, contra-rotating propellers, frozen rotor technique, OpenFOAM

1. Introduction

A smart and sustainable mobility is a relevant objective of the Horizon 2020 European Program. This goal goes through a more efficient use of the energy which will imply first a reduction of the fuel consumption, and consequently a reduction of the greenhouse gas emission. In addition, a contemporary reduction of the noise level has to be pursued. In order to meet these strong environmental requirements, new models of regional air transport systems have been developed based on novel concepts of vehicle equipped with a hybrid propulsion. Concerning Remotely Piloted Aerial Vehicles (RPAV), multi-rotors have been widely investigated since they can be easily arranged in different ways, due to the simpler mechanics, so as to be integrated with electric motors. A special class of multi-rotors is represented by the

* Corresponding author. Address: University of Salento, Dep. of Engineering for Innovation, Research Center for Energy and Environment (UNISALENTO-DII-CREA), Via per Monteroni, LECCE I-73100, Italy. Tel: +39 0832297759.

E-mail addresses: mariagrazia.degiorgi@unisalento.it (Maria Grazia De Giorgi)., teresa.donateo@unisalento.it (Teresa Donateo)., antonio.ficarella@unisalento.it (Antonio Ficarella)., donato.fontanarosa@unisalento.it (Donato Fontanarosa)., annaeva.morabito@unisalento.it (Anna Eva Morabito)., luca.scalinci@gmail.com (Luca Scalinci).

1876-6102
Peer-review under responsibility of the scientific committee of the 72nd Conference of the Italian Thermal Machines Engineering Association
10.1016/j.egypro.2017.08.273

Contra-Rotating Open Rotor (CROR) system. It consists of two coaxial propellers which are rotating in opposition in an open rotor configuration. The main advantage ot this kind of propulsive configuration lies in an increased propulsive efficiency coupled with a simpler design.

Coaxial rotors have been largely investigated. Concerning the numerical works, recently Heinrich et al. [1] investigated a new concept of advanced turbofans which consisted of a gearless one-motor contra-rotating fans. In particular they compared experimental data coming from a 2D Particle Image Velocimetry analysis, with numerical results coming from both a steady state model based on the frozen rotor technique, and unsteady and based on the Sliding Mesh (SM) approach. Under normal operating conditions results showed a good agreement between experiments and both quasi-steady and transient simulations. Close to stall, the last ones produced better predictions with respect to the steady state model. Xu et al. [2] estimated the performance of a ducted twin counter-rotating propeller system for a new concept of a Vertical Take-Off and Landing (VTOL) vehicle. Regarding the advancements of open rotor systems, a significant contribution to the understanding of the interference losses and differences in thrust between the upper and lower rotors were provided by Syal and Leishman [3] and Barbely et al. [4], who applied theoretical methods and the actuator disk modeling respectively. A similar numerical investigation was achieved by Lakshminarayan and Baeder [5] who performed RANS simulations. Recently, Yoon et al. [6] introduced a hybrid turbulence model into the numerical model in order to predict the effects of inter-rotor spacing and fuselage on the performance of coaxial rotor systems. Then, in Yoon et al. [7] the effects of torque balancing were investigated by solving the unsteady RANS (URANS) equations on overset grids coupled with high-order accurate schemes, dual-time stepping and the same hybrid turbulence model.

The present work focused on the numerical prediction of the performance of a CROR system, which is part of a hybrid propulsion system of a novel concept of convertible VTOL airplane called LeSR [8], i.e. Long endurance Small Range vehicle. The maximization of the propulsive efficiency of the CROR system is an essential issue of the design process in compliance with the long endurance requirement. In particular, a numerical CFD study has been conducted on a dual coaxial contra-rotating propellers system by using a frozen rotor technique. The open source code OpenFOAM has been used for computations. The axial distance between the front and the rear propellers was assumed a design constraint owing to the arrangement of electric motors. The present work aims to provide a performance analysis of a CROR system characterized by a relevant axial distance and a variable pitch. It was performed by varying the pitch configuration and the angular velocity of the rear propeller, for a given angular velocity of the front propeller. The analysis was strengthened by comparing results with the performance of a single propeller configuration and an equivalent dual non-coaxial counter-rotating propellers system.

2. Numerical methods

The open source CFD toolbox OpenFOAM© Version 2.1.1 was used for numerical simulations, based on a Finite Volume formulation.

2.1. Numerical model

The numerical model is based on the Frozen Rotor (FR) technique, which computes a steady-state solution of the Reynolds Average Navier-Stokes (RANS) equations for one rotor position. The FR technique neglects all time-dependent effects and flow instabilities, such that it is suited for investigation on the energetic performances of the system. It combines fast computations with a good accuracy of results. The FR technique uses a Multiple Reference Frames (MRF) model in order to solve the RANS equations in multiple sub-domains characterized by a specific reference frames. The MRF formulation applied to rotating flows separates rotating zones, which are generally referred to as rotors, with respect to the stationary zones, usually called stators. In our investigation a MRF zone is associated to the region near each propeller. Conversely, the outer domain is considered stationary, as shown in Fig. 1. At each iteration step the solution is patched between two adjacent different zones by means of an Arbitrary Mesh Interface (AMI), which allows for the exchange of the information. In particular, the FR technique assumes the same absolute velocity on both sides of the interface and therefore for each reference frame. Consequently the relative velocity $\mathbf{u_R}$ used for computations in the rotating zone, and the absolute velocity $\mathbf{u}$ used for computations in the stator zone, are related as follows

$$\mathbf{u_R} = \mathbf{u} - \mathbf{\Omega} \times \mathbf{r} \tag{1}$$

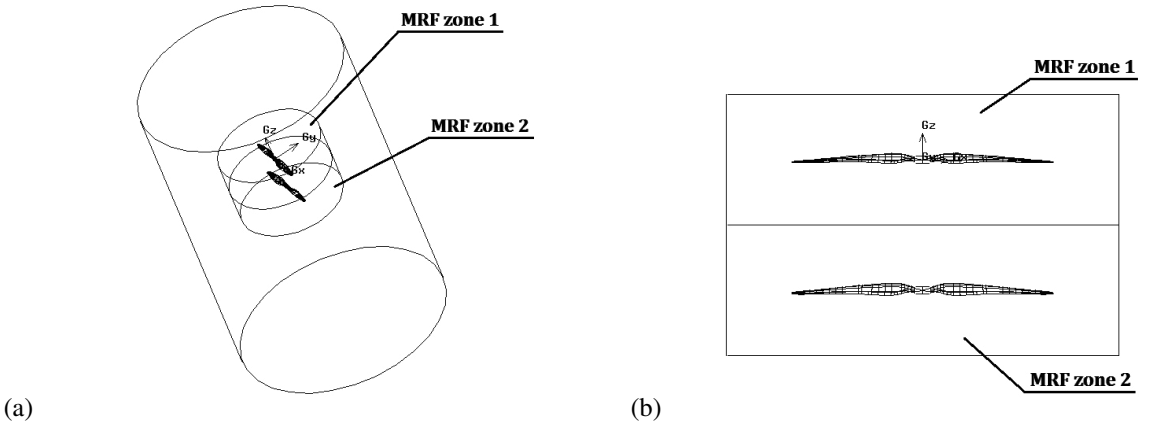

Fig. 1: Multiple Reference Frame zones for the CROR system: (a) enlarged view; (b) focused view.

where $\mathbf{\Omega}$ is the angular velocity of the rotating frame, and $\mathbf{r}$ is the radial vector.

The flow field satisfies the Mach number condition $M < 0.3$ almost everywhere, except a narrow region close to the tip of blades where compressibility effects rise as the flight conditions become severe. In the most critical conditions corresponding to a rotational speed of the propeller equal to 7000rpm and a tip Mach number equal to 0.43, we got a Mach number higher than 0.3 into 3.92% of the total cells in case of the single propeller, and 3.41% of the total cells in case concerning the contra-rotating configuration. The quantification of the numerical error affecting the incompressible flow predictions is far from the scope of the present work, which aims to a preliminary estimation of the performance of the contra-rotating propellers system. In this context, the airflow was supposed incompressible so as to simplify the numerical model thus given by the set of the governing equations expressed in Eqs. (2) and (3)

$$\nabla \cdot \mathbf{u} = 0 \tag{2}$$

$$\frac{D\mathbf{u}}{Dt} = -\nabla\left(\frac{p}{\rho}\right) + (\nu + \nu_t)\nabla^2\mathbf{u} \tag{3}$$

where ρ denotes the density, p the static pressure, $\mathbf{u}$ is the Reynolds-Averaged absolute velocity, ν and ν_t are the molecular and the turbulent kinematic viscosities respectively. In OpenFOAM the FR technique is based on the steady-state segregated solver called *simpleFoam*, which is based on the Semi-Implicit Method for Pressure Linked Equations (SIMPLE) algorithm. This solver is coupled with MRF sources, which introduce centrifugal and Coriolis forces in the rotating MRF zones. The Spalart-Allmaras model was used in order to consider the effects of the turbulence. Consequently the modified turbulent kinematic viscosity $\tilde{\nu}$ was introduced in the model.

The convective terms in transport equations were discretized by using the linear interpolation scheme for $\mathbf{u}$, and the linear upwind interpolation scheme for turbulent fields. Gradients were computed with the central differencing scheme. The convergence of computations was monitored by means of the final residuals. Simulations stopped just when the steady condition was reached for the thrust force T.

2.2. Computational domain, boundary conditions (BCs) and numerical setup

The computational domain and its boundaries are shown in Fig. 2 for both the single propeller and the CRP configuration. The geometry has been meshed by means of the commercial tool GAMBIT. A multi-block meshing strategy was used in order to distinguish rotor zones of propellers, from the stationary outer sub-domain. Each block is composed of unstructured tetrahedral elements. A single propeller block consists of a cylindrical sub-domain having a diameter of $1.5D_p$, where D_p is the diameter of the propeller, and a length of $0.25D_p$ upstream and $0.25D_p$ downstream. The outer domain has a diameter of $3.0D_p$ and a length of $1.5D_p$ upstream. Downstream the length is $2.5D_p$ in case of the single propeller configuration, and $3.0D_p$ for the CRP configuration. The mesh volumes were generated by applying the inflation method which makes use of a size function. As shown Fig. 3, the inflation method allowed to get a non-uniform mesh which is refined in the proximity of the propeller where strong gradients are expected. The

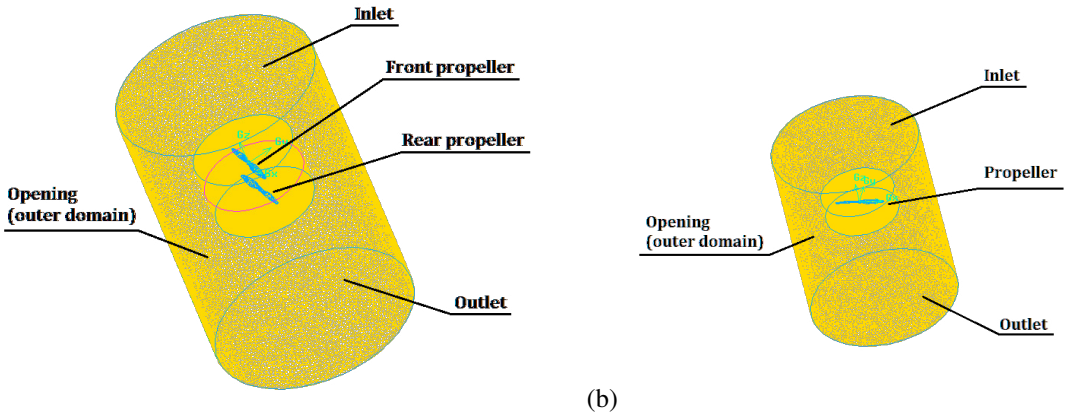

Fig. 2: Computational domain and boundaries: (a) single propeller configuration; (b) contra-rotating propellers (CRP) configuration.

size function is properly set by means of two sizing parameters, i.e. the growth rate and the maximum size. They were set at 1.5 and 10 for propeller zones, and 1.5 and 30 in case of the outer domain. The overall size of the 3D mesh is

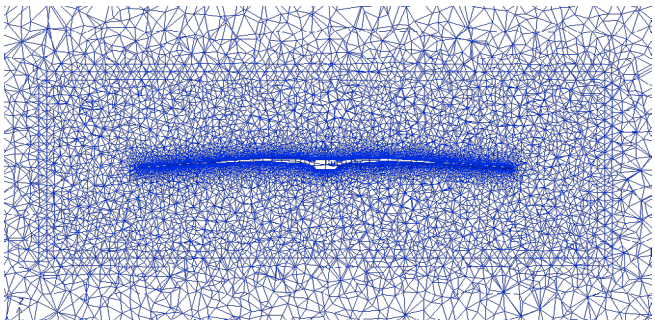

Fig. 3: Detailed view of the mesh refinement near the propeller.

a function of the refinement level of the mesh of the propeller's surface, which were meshed by means of the *pave* meshing scheme in combination with an Interval Size Parameter (ISP) properly set. This last term is defined as the ratio between the edge length L_{edge} and the resulting number of elements of the meshed edge n_{elem}.

The airflow properties were set by considering the International Standard Atmosphere (ISA) at sea level conditions, i.e. at temperature of 288 K and pressure of 101 325 Pa. Boundary conditions were defined for the inlet velocity, the pressure outlet. the turbulent kinematic viscosity and modified turbulent viscosity. The no-slip condition was imposed at walls. The flow was supposed axial, i.e. normal to the propeller disc. A summary of the boundary conditions is collected in the Table 1. The maximum y^+ computed on the propeller's surface was 12 during the entire numerical

Table 1: Boundary conditions in OpenFOAM.

Boundary	p	**U**	ν_t	$\tilde{\nu}$
Inlet	*zeroGradient*	*fixedValue*	*fixedValue*	*zeroGradient*
Outlet	*totalPressure*	*zeroGradient*	*fixedValue*	*zeroGradient*
Opening	*zeroGradient*	*zeroGradient*	*fixedValue*	*zeroGradient*
Propeller(s)	*zeroGradient*	*noSlip*	*nutkWallFunction*	*zeroGradient*

investigation.

The present work investigated the performances of different propeller systems, by providing a numerical estimation of the coefficients of thrust and power, denoted by C_T and C_P, and the propulsive efficiency η_p. They are defined as follows:

$$C_T = \frac{T}{\rho n_1^2 D_p^4}\,, \quad C_P = \frac{P_{ax}}{\rho n_1^3 D_p^5}\,, \quad \eta_p = \frac{T V_i}{P_{ax}} = \frac{C_T J}{C_P} \quad \text{with} \quad J = \frac{V_i}{n_1 D_p} \tag{4}$$

where T is the propeller thrust, P_{ax} is the power required to rotate the propeller, V_i is the inlet velocity and n_1 is the angular velocity of the main propeller.

3. Results and discussion

In order to evaluate the performance of the CROR system, comparisons were performed between three different propeller configurations: the mono-propeller case, the contra-rotating propellers case and a counter-rotating propellers case. The last one consists of two identical propellers rotating in the same direction, located at an infinite distance and placed in parallel to each other. The performance of a bi-propellers system has been evaluated as shown in Eqs. (5).

$$C_{T,eq} = \frac{T_1 + T_2}{\rho n_1^2 D_p^4} = C_{T1} + C_{T2}\,, \quad C_{P,eq} = \frac{P_{ax,1} + P_{ax,2}}{\rho n_1^3 D_p^5} = C_{P1} + C_{P2}\,, \quad \eta_{p,eq} = \frac{(T_1 + T_2) V_i}{P_{ax,1} + P_{ax,2}} = \frac{(C_{T_1} + C_{T2}) J}{C_{P,1} + C_{P_2}} \tag{5}$$

In case of counter-rotating propellers, last equations lead to $C_{T,counter} = 2C_T$, $C_{P,counter} = 2C_P$, and $\eta_{p,counter} = \eta_p$.

3.1. Evaluation of the numerical model

The Grid Independence Study (GIS) was performed in order to define the ISP to be used for meshing each propeller zone. To this end, several simulations were run by considering one single propeller at $n_1 = 6000$ rpm, $p_1 = 0.1397$ m = 8.30° and for an advance ratio of 0.4. Table 2 shows that the independence of the grid was reached for the middle refinement of the mesh, which is composed of 2.47 million cells obtained using an ISP equal to 0.6. It corresponds to a thrust $T = 8.770$ N and a torque $Q = 0.405$ N m.

Table 2: Grid Independence Study: results.

Refinement Level	**ISP [-]**	**Mesh Size [million cells]**	**Thrust, T N**	**Torque, Q Nm**
Coarse	1.8	1.56	8.703	0.408409
Middle	0.6	2.47	8.770	0.405000
Fine	0.4	3.92	8.789	0.405388

In order to evaluate the behavior of the implemented numerical model, the OpenFOAM results of the single propeller were compared to the numerical data provided by the manufacturer coming from the Vortex Theory [9]. Table 3 shows η_p and C_T and the relative deviation, at $J = 0.1, 0.2, 0.3, 0.4$.

Table 3: Comparison with Vortex Theory. OF: OpenFOAM results; Vortex Theory: data provided by the manufacturer.

		η_p[-]			C_T[-]		
		OF	**Vortex Theory**	Δ_{rel}	**OF**	**Vortex Theory**	Δ_{rel}
J [-]	**0.1**	0.263	0.275	0.044	0.0586	0.0820	0.275
	0.2	0.463	0.495	0.065	0.0505	0.0690	0.263
	0.3	0.573	0.651	0.120	0.0369	0.0537	0.268
	0.4	0.560	0.743	0.246	0.0263	0.0363	0.285

Fig 4 shows a similar increasing trend of C_T and η_p for both models with respect to the advance ratio J. On the contrary, the trend for η_p is different for high values of J. Solid black lines represent CFD computation, while dashed

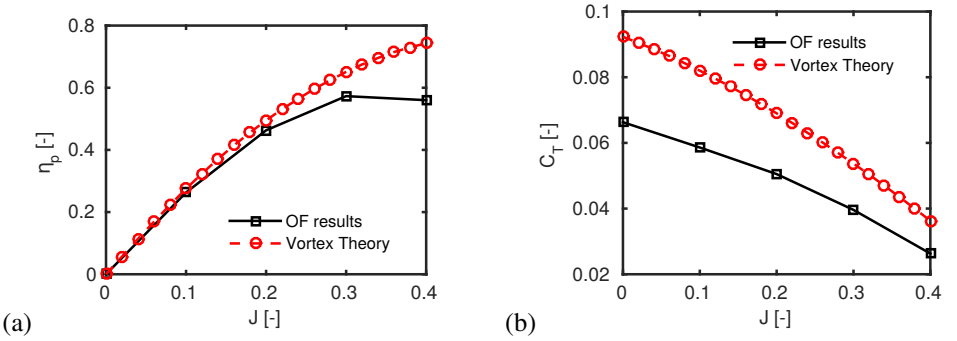

Fig. 4: Comparison curves: (a) $\eta_p - J$; (b) $C_T - J$.

red lines refer to the Vortex Theory's data. Comparisons highlight that the OpenFOAM model underestimates the performance with respect to the Vortex Theory model. The CFD prediction of the propulsive efficiency well matches that aroused out of the Vortex Theory in the range of $J \leq 0.3$ with a deviation less than 15%. As the advance ratio increases to $J = 0.4$, the deviation between the estimations coming out of the models grows up to 24.6%. Concerning the prediction of the thrust, the underestimation provided by the CFD model with respect to the Vortex Theory model remains approximately constant and equal to about 27% regardless of the value of J.

3.2. Performance analysis

Two sets of simulations were carried out. The first one concerned the contra-rotating propellers configuration at $J = 0.4$. Fixed the angular velocity of the front propeller at $n_1 = 6000$ rpm and its pitch at $p_1 = 0.1397$ m $= 8.30°$, simulations were performed by varying the operating conditions, defined by means of the pitch p_2 and the angular velocity n_2 of the rear propeller. Both p_1 and p_2 were defined with respect to the station at the 75% of the blade. Table 4 shows the test matrix of this first set of computations. In the second set of simulations, the flight condition,

Table 4: Test matrix. Notes: the pitch of the propeller is referred to the station at the 75% of the blade

		p_2					
		0.1397m (8.30°)	**0.1524m (9.04°)**	**0.1778m (10.52°)**	**0.2032m (11.98°)**	**0.254m (14.86°)**	**0.3048m (17.66°)**
n_2 [rpm]	**4000**					SIM1	SIM2
	5000	SIM3	SIM4	SIM5	SIM6	SIM7	SIM8
	6000	SIM9	SIM10	SIM11	SIM12	SIM13	
	7000	SIM14	SIM15	SIM16	SIM17	SIM18	

which corresponds to a specific advanced ratio J, was varied for fixed operating conditions of propellers. In particular, computations were performed at $n_2 = 5000$ rpm and $p_2 = 0.254$ m $= 14.86°$.

The comparison between the contra-rotating system and the equivalent counter-rotating system is represented in Fig 5, which shows the propulsive efficiency η_p and the thrust T as a function of the pitch of the rear propeller p_2 for different rotational speed n_2 at $J = 0.4$. The thrust of the contra-rotating system grows as p_2 increases for fixed n_2 and J. The rotational speed of the rear propeller determines the slope of the curve $T - p_2$, which rises as n_2 increases. Therefore, the more n_2 is, the more convenient it would be to use the contra-rotating configuration. However, the most efficient operating condition is obtained at $n_2 = 5000$rpm and $p_2 \in [0.254\,\text{m} \div 0.3048\,\text{m}] = [14.86° \div 17.66°]$, as shown by the relation $\eta_p - p_2$ at fixed n_2 and J. These findings strongly depends on the flight condition represented by J, p_1 and n_1, and to a lesser extent on the distance between the front propeller and the rear propeller. They determine how much energy of the flow swirling downstream the front propeller is exploited by the rear propeller, which straightens the flow downstream as highlighted in the Fig. 6. This figure shows the streamlines of the flow for the contra-rotating

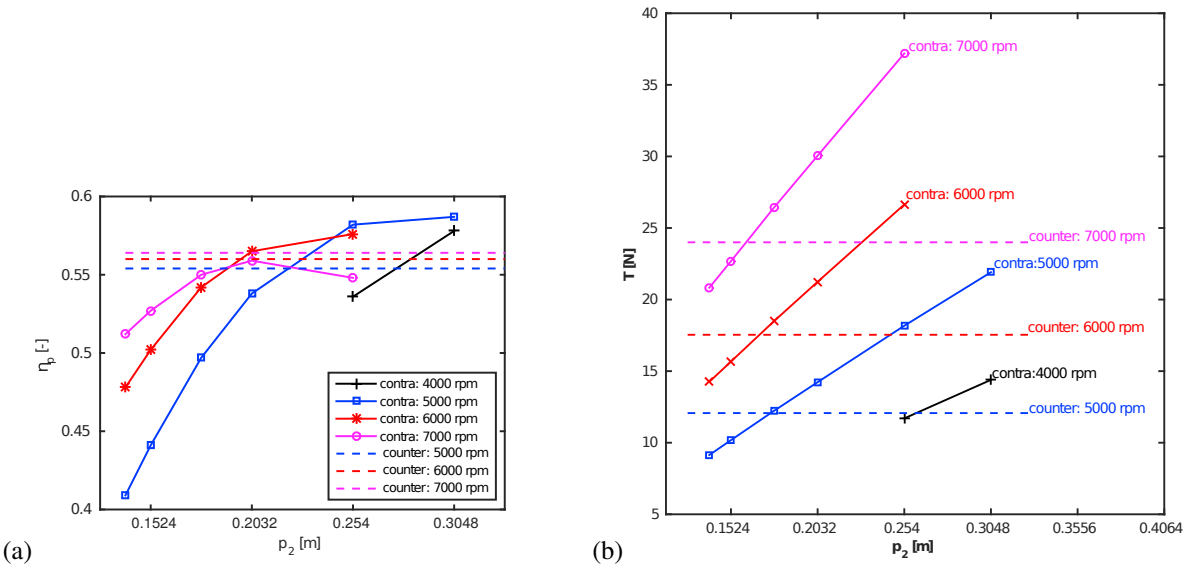

Fig. 5: Performances as a function of the pitch at $J = 0.4$: (a) propulsive efficiency, η_p; (b) thrust, T. Dual contra-rotating (contra) at $n_1 = 6000$rpm, $p_1 = 0.1397\,\text{m} = 8.30°$ and $p_2 = 0.254\,\text{m} = 14.86°$, for different values of n_2. Dual counter-rotating (counter) at $p_2 = p_1 = 0.1397\,\text{m} = 8.30°$ for different values of $n_2 = n_1$.

configuration (Fig. 6(a)) with respect to the single propeller configuration (Fig. 6(b)), as seen by the an observer sited downstream in front of the rear propeller.

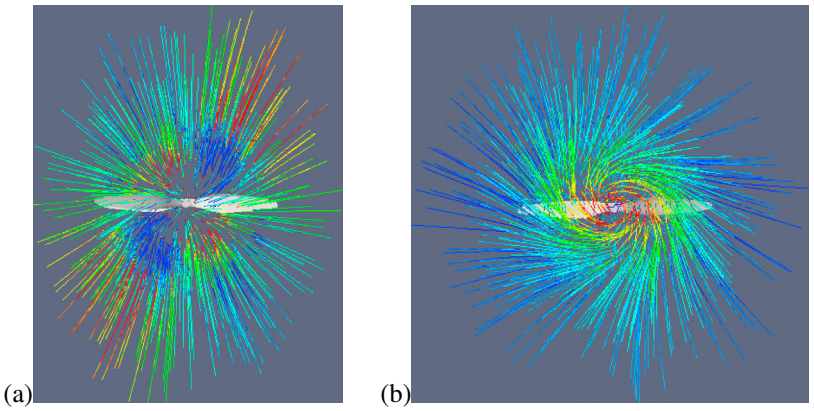

Fig. 6: Rear view of the air flow streamlines: (a) contra-rotating configuration at $J = 0.4$, $n_1 = 6000$rpm and $p_1 = 0.1397\,\text{m} = 8.30°$, $n_2 = 5000$rpm and $p_2 = 0.254\,\text{m} = 14.86°$ (SIM7); (b) single propeller configuration at $J = 0.4$, $n_1 = 6000$rpm and $p_1 = 0.1397\,\text{m} = 8.30°$. Colors of the streamlines represent the vorticity along the z-axis. Notes: pictures have not the same color scale.

In Fig. 7 the performances of the contra-rotating system are compared with those concerning the equivalent counter-rotating system, as a function of the advance ratio J. Starting from the previous considerations, the pitch of the rear propeller has been set to equal to $p_2 = 0.254\,\text{m} = 14.86°$. The propulsive efficiencies (Fig. 7(a)) highlight that the contra-rotating propellers system has a broader operational range of J, even thought there is no advantage in term of magnitude. The power and thrust coefficients are shown in Fig. 7(b). Except the low velocity range ($J \in [0 \div 0.1]$) where the contra-rotating system exhibits a worse power coefficient C_P than the counter-rotating system, then they are almost equivalent. Instead, the trends of the thrust coefficient C_T confirm that the contra-rotating configuration is suitable in the range of the high advanced ratios $J \geq 0.4$.

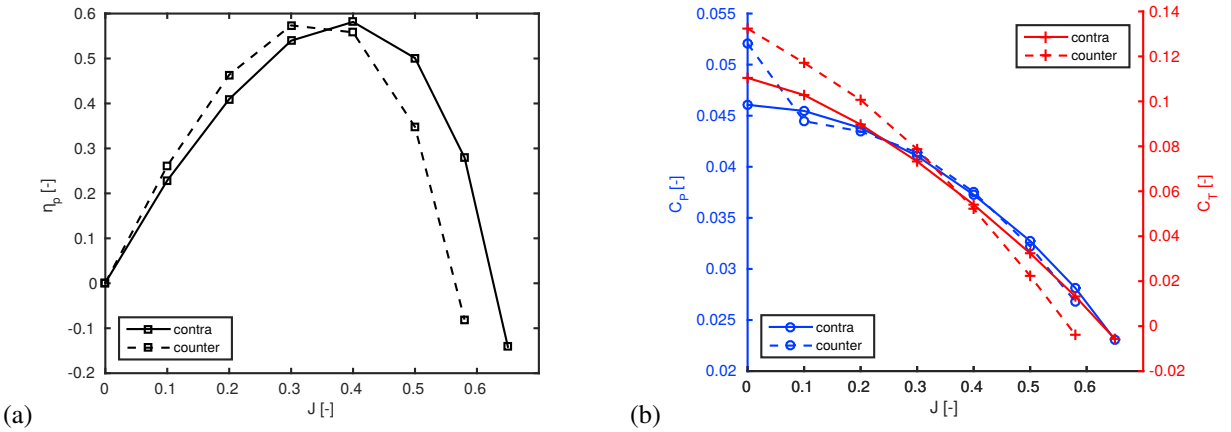

Fig. 7: Performances as a function of the advance ratio: (a) propulsive efficiency; (b) thrust (red) and power (blue) coefficients. Dual contra-rotating (contra) at $n_1 = 6000$rpm, $n_2 = 5000$rpm, $p_1 = 0.1397\,\mathrm{m} = 8.30°$ and $p_2 = 0.254\,\mathrm{m} = 14.86°$. Dual counter-rotating (counter) at $n_2 = n_1 = 6000$rpm and $p_2 = p_1 = 0.1397\,\mathrm{m} = 8.30°$.

4. Conclusions and future works

The present work showed the performance analysis of a Contra-Rotating Open Rotor system by means of a CFD investigation. In order to evaluate the predicted behavior of the contra-rotating system, the investigation also concerned the single propeller and an equivalent counter-rotating system. The influence of the angular velocity and the pitch of the rear propeller was estimated, as well as the effect of the advance ratio. It was found that the contra-rotating configuration is preferred in case of larger pitch and higher advance ratio. In particular, a relevant increase of thrust, an improvement of the propulsive efficiency and a broader operational range of flight condition were predicted.

Next step will be a new broader investigation aimed at a deeper understanding of the behavior of the CROR system. The improvement of the comparison of numerical results with data provided by the manufacturer will be an essential requirement. This purpose will pass through a better reconstruction of the geometry, as well as the implementation of a more accurate turbulence model.

References

[1] M. Heinrich, C. Friebe, R. Schwarze, Experimental and numerical investigation of a gearless one-motor contra-rotating fan, Proceedings of the Institution of Mechanical Engineers, Part A: Journal of Power and Energy 230 (5) (2016) 467–476.

[2] C. Xu, C. Bil, S. C. Cheung, Fluid dynamics analysis of a counter–rotating ducted propeller, in: 29th Congress of the International Concil of the Aeronautical Sciences, 2014.

[3] M. Syal, J. G. Leishman, Aerodynamic optimization study of a coaxial rotor in hovering flight, Journal of the American Helicopter Society 57 (4) (2012) 1–15.

[4] N. L. Barbely, N. M. Komerath, L. A. Novak, A study of coaxial rotor performance and flow field characteristics, in: American Helicopter Society Aeromechanics Specialists Conference, San Francisco, CA, 2016.

[5] V. K. Lakshminarayan, J. D. Baeder, High-resolution computational investigation of trimmed coaxial rotor aerodynamics in hover, Journal of the American Helicopter Society 54 (042008) (2009) 21 pp.

[6] S. Yoon, H. C. Lee, T. H. Pulliam, Computational study of flow interactions in coaxial rotors, in: AHS Technical Meeting on Aeromechanics Design for Vertical Lift; 20-22 Jan. 2016; San Francisco, CA; United States, no. ARC-E-DAA-TN24718, NASA Ames Research Center; Moffett Field, CA United States, 2016, p. 8 pp.

[7] S. Yoon, W. M. Chan, T. H. Pulliam, Computations of torque-balanced coaxial rotor flows, in: 55th AIAA Aerospace Sciences Meeting, no. AIAA 2017-0052, 2017.

[8] P. Miodushevsky, Convertible airplane, uS Patent App. 13/743,763 (Oct. 10 2013).
URL `https://www.google.ch/patents/US20130264429`

[9] B. .Brandt, R. W. Deters, G. Ananda, M. Selig, Uiuc propeller database (May 2017).
URL `http://m-selig.ae.illinois.edu/props/propDB.html`